Development of a large active area beam telescope based on the SiD microstrip sensor☆

Mengqing Wu[a,*], Martin Breidenbach[b], Dietrich Freytag[b], Ryan Herbst[b], Uwe Kraemer[a], Benjamin Reese[b], Sebastiaan Roelofs[c], Marcel Stanitzki[a]

[a] *Deutsches Elektronen-Synchrotron DESY, Notkestr. 85, 22607 Hamburg, Germany*
[b] *Stanford Linear Accelerator Center SLAC, 2575 Sand Hill Road, Menlo Park, CA 94025 USA*
[c] *The Hague University of Applied Sciences, Rotterdamseweg 137, 2628 AL Delft, The Netherlands*

Abstract

A beam telescope as one of the most important and often requested test beam equipment provides particle tracking to test beam users. At the DESY II test beam facility, a new beam telescope called Lycoris based on a microstrip sensor has been designed to address the user demands for momentum measurement in a 1 T solenoid magnet or large area tracking with limited space (3.5 cm between the potential user device and the magnet inner wall). Lycoris is designed to provide a high-precision resolution of at least ~10 μm along the bending direction, and a large active area of 10×10 cm^2 to cover at least 90% of the beam particles at energies of 1-6 GeV. The microstrip sensor was originally designed for the Silicon Detector (SiD) at the International Linear Collider (ILC), which adopted a hybrid-less design, i.e. a second metallization layer is used to route signals from strips to the bump-bonded ASIC, and from the ASIC to a wire-bond pad to the outside. This hybrid-less arrangement eliminates the need for a complex hybrid design, and its functioning is first-time tested in this project. The performance of the sensor modules was firstly tested in the lab then at the DESY II test beam facility in August/September 2018, and the results will be presented here. In addition, a summary will be given at the end with an overview of the ongoing test beam campaign of the Lycoris prototype in February 2019.

Keywords: Silicon Strip Sensor, Hybrid-less readout, Beam telescope tracker, DESY II test beam facility

1. Introduction

Test beam and irradiation facilities are the key infrastructures for research in high-energy physics detectors, and a beam telescope is one of the most important test beam infrastructure for particle tracking. At the DESY II test beam facility [1], there has been the request by the user community, to install an external beam telescope inside the PCMAG 1 T solenoid, providing precise tracks covering a large area and at the same time fitting into the small area (~3.5 cm) between the potential device under test (DUT) and the inner wall of the magnet.

A six-layer beam telescope named Lycoris has been designed with two arms of three layers each, and each layer consists of two microstrip sensors side-by-side along the magnetic field. Each arm is integrated into one unit by a compact aluminium box, called cassette, see Fig. 1. Lycoris provides a spatial resolution better than 10 μm along the bending direction for achieving a momentum resolution better than 2×10^{-5} GeV^{-1}, a time resolution configurable as multiples of 80 ns, flexible stereo angle configurations of 0°, 2°, or 90°, and a large active area of 10×10 cm^2 (10×20 cm^2) to cover 90% to 96% of the beam particles with energies from 1 to 6 GeV.

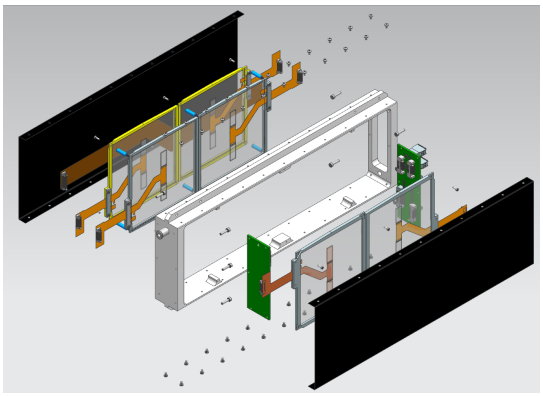

Figure 1: CAD drawing of each component of one arm of the telescope. Three layers of two side-by-side sensors will be installed in an aluminium cassette-like support (3.3 cm thick, 12.1 cm high, and 32.1 cm long) covered by two carbon fibre windows, at each endplate of the cassette, a local readout electronic support is installed for power and digital communication.

2. Sensor Module

Hybrid-less microstrip sensor. The microstrip sensor module is ~10×10 cm^2 large and 320 mm thick, with a 25 μm(50 μm) sense (readout) pitch providing an expected spatial resolution in theory of ~7.2 μm. It was originally designed for the SiD Detector Concept for the ILC [2]. The sensors were produced by Hamamatsu, all showing very good electric features, i.e. a few hundreds nA leakage current and all depleting at around 50 V.

*Corresponding author
Email address: mengqing.wu@desy.de (Mengqing Wu)

This sensor is readout by two bump-bonded 1024-channel KPiX [3] ASICs, through a second metallization layer. Each KPiX digitizes signals from 920 strips with a 13-bit ADC, then serializes and sends out data through the second metallization layer to a wire-bonded Kapton cable, see Fig. 2. Such an arrangement is also used for powering KPiX and transmitting other digital signals such as command, clock and trigger. This hybrid-less concept eliminates the need for a complex hybrid design, and its functioning is first-time tested in the LYCORIS project.

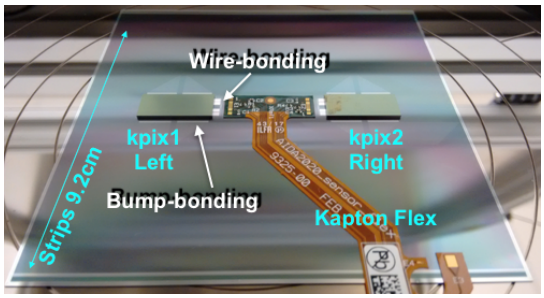

Figure 2: Photo of an assembled sensor module.

KPiX Readout ASIC. The KPiX chip employs a power cycle design, i.e. the chip will receive a power-on pulse to be active for a certain period of time called *acquisition cycle*, then powered off. This feature lowers the average power dissipation and thus making gas cooling feasible to further reduce the material budget. The acquisition cycle, is configurable based on a 100 MHz clock during which each readout channel can store up to four events. The chip is able to run with self-triggers or with external triggers sent out from a trigger logic unit (TLU), additionally, it can timestamp the external triggers to study the self-trigger efficiency.

The KPiX readout system was tested with hexagonal pixel sensors developed for the SiD ECAL [2, 3]. This ECAL sensor was later used as a reference device in the first test beam campaigns for the LYCORIS project.

3. Commissioning Tests

Lab Test. The sensor module was firstly tested in the lab without the cassette. The test setup was installed in a grounded aluminium dark box, to provide a relatively noise-free environment. Various data taking modes were tested in the lab, including channel-by-channel ADC calibration, forced trigger pedestal measurement, self-trigger noise and signal runs.

ADC calibration is done by a preicision calibrator of the chip for every channel, which sends out amplitudes and timings according to configurations. An 8 bit DAC is used to provide 256 calibration values with each defined to a precision of 12 bit [3]. Under the gain used in this study, each DAC injects a charge of 1 fC for the first 10 fC and later 2 fC (~ 12500 electrons). A slope to convert the ADC response to fC (or number of electrons) can be determined by performaing a linear fit on the ADC response against DAC for each channel.

One can determine the intrinsic noise level of each channel, by recording random noise with a forced trigger configuration. A preliminary average noise level of ~0.5 fC is determined from the distribution of the RMS of all the channels' response in a pedestal run, see the black histogram in Fig. 3.

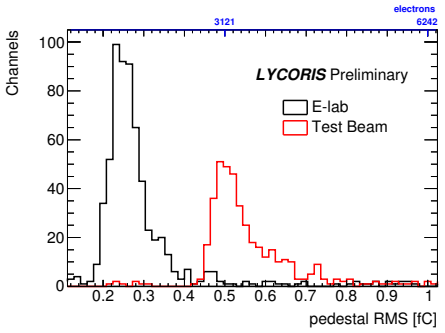

Figure 3: RMS of charge response in fC of all the channels in one KPiX measured from forced trigger run, where the black histogram refers to the lab measurements and the red refers to the test beam results.

Testbeam Test. The DESY II Test Beam Area T24 and its infrastructure [1] were used for the test beam campaign in August/September 2018. This was the first sensor module test beam qualification campaign and the two ASICs were tested separately. The beam energy was chosen to be 3 GeV to achieve the best beam rate, and a $9 \times 9\,\mathrm{mm}^2$ secondary collimator was chosen. The trigger rate was measured to be ~5 kHz during the data taking period of KPiX. See the test setup in Fig. 4, it is similar to the one in the lab, but with the following differences:

- The sensor module was held in the cassette which provides better shielding;
- One SiD ECAL sensor was placed behind the sensor module as a reference device;
- Two scintillators installed between the secondary collimator and the sensor module, feed coincidence signals to the KPiX readout system as an external trigger source.

All the readout channels were re-calibrated due to the changes in the experimental setup and environment, and as expected, the ADC to fC slopes stayed the same as the lab measurements. The pedestal measurement was repeated as well, and the noise level measured is lowered at ~0.28 fC as expected from a better-shielded environment with the grounded cassette, see the red histogram in Fig. 3.

4. Performance results

Self-trigger. Under the self-trigger mode, only channels with a signal above a certain threshold will be readout. Background rejection can be done by increasing the threshold, but in the meanwhile signal efficiency also goes down. One efficient way to suppress noise events is to match self-triggered events with external triggers. This can be done by comparing timestamps

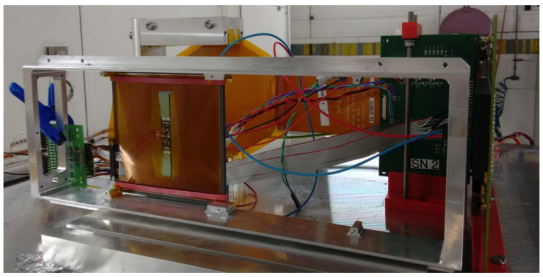

Figure 4: Experimental setup at the DESY II Test Beam Area T24 in August/September 2018, with the strip sensor module in front and the reference ECAL pixel sensor behind.

from the self-triggers to the external triggers. Timestamps are recorded based on a 13 bit local clock counter called BunchClkCount. This timing feature has been studied before with the ECAL sensor [4], while this is the first time to study it on the microstrip sensor. Fig. 5 shows the distribution of time difference ΔT from self-triggered events to the external triggers, where an expected time offset of 1-2 BunchClkCounts is observed for both sensors due to the internal circuitry delay for signal amplification and trigger. The strip sensor module shows a different feature, that some events triggered after the expected timestamp offset with a fixed period equal to the trigger reset time of 8 BunchClkCounts. These events are believed to be events retriggered from the neighbour channels due to the large current induced during the trigger reset.

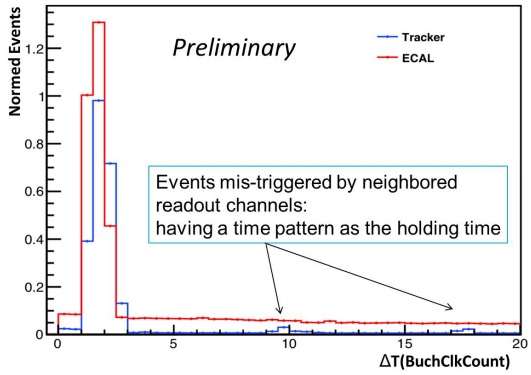

Figure 5: Distribution of time difference ΔT from self-triggered events to the external triggers, in *BunchClockCount* (a count based on the data taking clock); all events from all the channels are plotted.

A criterion of $0 < \Delta T < 3$ is applied to select events that match with an external trigger, called *time-correlated events*. Fig. 6 shows the ADC distribution recorded from one example strip in the beam. The purity of the time-correlated events is demonstrated by the fact that the distribution of the time-correlated events (red histogram) very well replicate the tail of the distribution of all the self-triggered events (blue histogram) and a reasonably good Landau fit can be performed on it.

Moreover, the sensor shows a good capability in locating the signal, see the signal response from time-correlated events distribution along the strip from the left half of the tested sensor Fig. 7. The signal area from strip #450 to strip #650 gives a

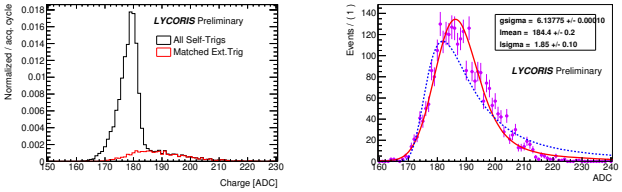

Figure 6: Charge response in ADC of one example strip in the beam of self-triggered data at the test beam. It includes a comparison plot (left) from events matched to external triggers in time (time-correlated events) to all the self-triggered events, and a zoom-in view of the time-correlated distribution (right) with a fit (red) on a Landau Gaussian convolution model and a fit (blue) on Landau only model.

good spatial response of ~10 mm (200×50µm) compatible with the beam size of $9 \times 9\,\mathrm{mm}^2$, demonstrating the functioning of this novel readout design. The blacked-out strips in the signal region are manually disabled due to calibration failures or high noise. More studies have to be done with more sensors and a refined system to get a more conclusive result.

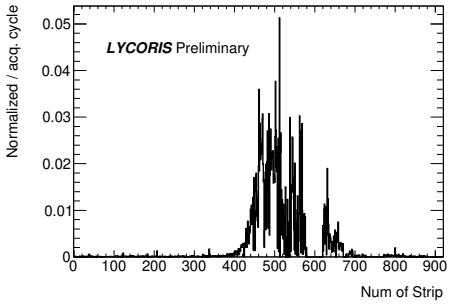

Figure 7: Signal response of the left half of the tested sensor from self-trigger data taken in the test beam with a very tight threshold, events shown here are time-correlated events. X-axis refers to the strip number, and entries are normalized showing how likely each strip is able to register one event per acquisition cycle. The blacked-out strips in the signal region are manually disabled because of bad calibration or high noise.

External-trigger. Every strip on the sensor will be readout once KPiX receives an external trigger, i.e. KPiX records signal response on top of the pedestal noise in the external-trigger mode. One needs to subtract pedestal in order to test the signal response. The subtraction is done channel by channel as the pedestal level varies from channel to channel as shown in Fig. 8. The pedestal for a channel is defined by the median from its fC response in order to be less affected by outliers. The *common mode* noise is also taken into account in the pedestal subtraction, which is found significantly shifting the pedestal level from cycle to cycle. This noise is calculated per channel as $\frac{1}{N}\sum_{i=0}^{N}(Raw_i - Pedestal_i)$, where N is number of acquisition cycles, Raw and Pedestal represents the raw and pedestal fC response of this channel respectively. Fig. 8 shows the charge response from the left half of the tested sensor in fC after pedestal subtraction from a noise run (upper) and from a signal run (lower) in the external-trigger mode. The noise run distribution is fitted with a Gaussian distribution, which gives a noise

level of 0.28 fC, comparable to the noise measurement shown in Fig. 3.

The signal data was first studied by applying thresholds on single strip charge after subtracting the pedestal according to two different hit profiles: hit on the floating strip and hit on the readout strip. These selected hits become seeds to form clusters in the preliminary hit cluster. This is now improved with the following clustering procedure:

- all the fired strips with $S/N > 3$ are classified as a hit candidate, where the noise level N is determined for each strip according to its charge response distribution after pedestal subtraction;
- all the hit candidates are input to a clustering algorithm, which iteratively looks for the most significant hit as the cluster seed and groups its neighbour hits to a hit cluster.

A tight cut is applied on clusters shown in Fig. 8 (lower) for purity by requiring significance ≥ 7, charge ≥ 2 fC and size (i.e. number of strips) smaller than 3. The spatial response from external trigger data is shown in Fig. 9 with selected signal events over the strips on the left half of the tested sensor, where the beam position and size is comparable as the self-trigger result shown in Fig. 7 demonstrating the functionality of the external trigger mode data taking.

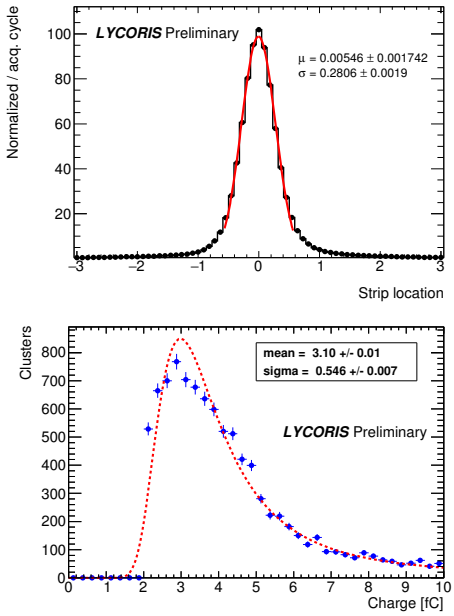

Figure 8: Response of half of the strip sensor in fC from external trigger data in noise run (upper) and in signal run (lower), pedestal subtraction applied. Extra cuts applied to the lower distribution, that only events with hit on floating strip is selected by requiring charge recorded from strips above 1 fC.

5. Summary

This is the first application of the SiD hybrid-less microstrip sensor. The sensor has been characterized and its designed feature such as the hybrid-less readout has been validated. The

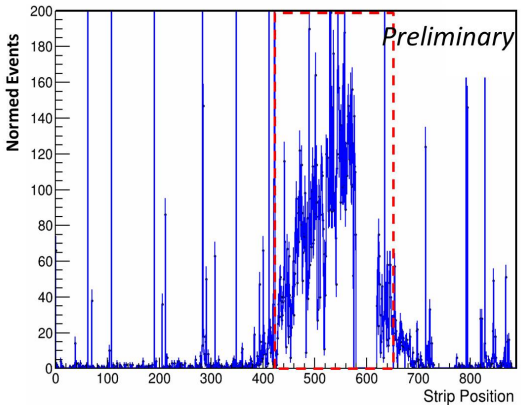

Figure 9: Number of hits plotted with respect to the centre of gravity of the hit cluster along the strip position. External trigger signal run data is used, with pedestal subtraction algorithm applied. The two hit profiles are both counted in the plot.

first test beam results from data collected at DESY II test beam facility in August/September 2018 shows a promising signal to noise ratio S/N of 10. This data demonstrates the signal response in terms of beam spot location and signal loss in a Landau shape, which is a very important study to confirm the functionality of this never tested sensor module with a novel readout design. It also reveals problems such as calibration failures and offset self triggers, which needs more tests on more sensors with a refined system including mechanical support and readout electronics to achieve more conclusive results. There are many designed features which will help to improve the performance but not applied in the data used in this paper, such as the humidity control and refined electronics in cabling, signalling and powering. This later turns out to largely cut off the calibration failures and suppress the noise level. Furthermore, software algorithm development also requires more data and statistics to verify, as a result, many improvements happened after the second test beam in February/March 2019, such as the clustering algorithm.

The test beam campaign in February/March 2019 was performed with two cassettes hosting one sensor module each, where the carbon fibre windows of the cassette were installed to improve the shielding. Analysis results on data from February/March 2019 show an improved S/N of ~15 with improved shielding and cabling, moreover, a good spatial correlation is found among the two sensor planes demonstrating the system's capability in tracking. More work is ongoing in developing clustering algorithm and tracking reconstruction. Two more test beam campaigns with the full six layers telescope configuration have been completed at DESY respectively in April and July 2019. The telescope was installed inside the PCMAG solenoid in these two test beams with an EUDET telescope [5] as the reference device, and the data was taken with and without the B-field.

Acknowledgements

This project has received funding from the European Unions Horizon 2020 Research and Innovation programme under Grant Agreement no. 654168. The authors would like to acknowledge Deutsches Elektronen-Synchrotron DESY and Helmholtz Gesellschaft Funding for all the support. The measurements leading to these results have been performed at the test beam facility at DESY Hamburg (Germany), a member of the Helmholtz Association. The authors would like to thank the technical team at the DESY II accelerator and test beam facility for the smooth operation of the test beam and the support during the test beam campaign.

References

[1] R. Diener, et al., The DESY II Test Beam Facility, Nucl. Instrum. Meth. A922 (2019) 265–286. arXiv:1807.09328, doi:10.1016/j.nima.2018.11.133.

[2] H. Abramowicz, et al., The International Linear Collider Technical Design Report - Volume 4: DetectorsarXiv:1306.6329.

[3] J. Brau, et al., Kpix - a 1,024 channel readout asic for the ilc, in: 2012 IEEE Nuclear Science Symposium and Medical Imaging Conference Record (NSS/MIC), 2012, pp. 1857–1860. doi:10.1109/NSSMIC.2012.6551433.

[4] U. Krmer, D. Tsionou, M. Stanitzki, M. Wu, LYCORIS - A Large Area Strip Telescope, in: International Workshop on Future Linear Collider (LCWS2017) Strasbourg, France, October 23-27, 2017, 2018. arXiv:1801.08505.

[5] H. Jansen, et al., Performance of the EUDET-type beam telescopes, EPJ Tech. Instrum. 3 (1) (2016) 7. arXiv:1603.09669, doi:10.1140/epjti/s40485-016-0033-2.